Hybrid Modeling of a Hall Thruster Using Hyperbolic System of Electron Conservation Laws

IEPC-2015-206／ISTS-2015-b-206

Presented at Joint Conference of 30th International Symposium on Space Technology and Science, 34th International Electric Propulsion Conference and 6th Nano-satellite Symposium
Hyogo-Kobe, Japan
July 4–10, 2015

Rei Kawashima[*], Kimiya Komurasaki[†], Tony Schönherr[‡], and Hiroyuki Koizumi[§]
The University of Tokyo, Tokyo, 113-8656, Japan

Abstract: The hyperbolic-equation system (HES) approach is applied to the calculation of a Hall thruster using the hybrid particle-in-cell (PIC) method. The HES approach enables accurate computations of magnetized electron fluids in quasi-neutral plasmas with a simple structured mesh. SPT-100 thruster is assumed as the calculation condition. The calculation results indicate that the Bohm criterion is satisfied for the channel walls. Also, the Boltzmann relation is confirmed in the region of strong magnetic confinement. These facts prove that the HES approach accurately calculates the boundary condition of wall sheath, and the characteristics of magnetized electron fluid in Hall thrusters.

Nomenclature

n_{e}	= electron number density
ϕ	= space potential
ϕ_{n}	= negative potential
u_{e}	= electron velocity
T_{e}	= electron temperature
g	= energy diffusion velocity
t_{p}	= pseudo time
ν_{ion}	= ionization collision frequency
ν_{col}	= total collision frequency
σ_{ion}	= ionization collision cross-section
σ_{col}	= total collision cross-section
$\varepsilon_{\mathrm{ion}}$	= first ionization energy
μ	= electron mobility
Γ	= number flux density
B	= magnetic flux density
α_{B}	= Bohm diffusion coefficient
u_{Bohm}	= Bohm velocity
ϕ_{th}	= thermalized potential
Subscripts	
s	= plasma-sheath boundary
w	= wall

[*]Graduate Student, Department of Aeronautics and Astronautics, kawashima@al.t.u-tokyo.ac.jp.
[†]Professor, Department of Aeronautics and Astronautics, komurasaki@al.t.u-tokyo.ac.jp.
[‡]Assistant Professor, Department of Aeronautics and Astronautics, schoenherr@al.t.u-tokyo.ac.jp.
[§]Associate Professor, Department of Advanced Energy, koizumi@al.t.u-tokyo.ac.jp.

I. Introduction

Hall thrusters are promising technology for high-power electric propulsion system which enables next-generation missions such as the manned Mars mission and solar power satellite. In such a situation, the important role of numerical simulations is the lifetime investigations. It is known that the factor of lifetime limitation is the channel wall erosions.[1] Since endurance tests for lifetime investigation is costly, the replacement of experiments by numerical simulations saves a lot of cost and time. A number of simulations have been conducted for the prediction of thruster lifetime[2] and reduction of wall erosions.[3]

Recently a technology named "magnetic shielding" has been proposed.[4] A significant reduction of channel wall erosion was observed,[5] and the mechanism of the technology has been investigated by numerical analyses.[6] The magnetic shielding utilizes concave magnetic lines of force toward downstream, which bypass the channel wall. The future numerical simulations for Hall thrusters should be capable of analyzing the complicated magnetic topology of the magnetic shielding.

In numerical simulations of Hall thrusters, the hybrid particle-in-cell (PIC) method has been the most popular approach owing to the validity of modeling and reasonable computational cost.[7] The hybrid model applies the fluid approximation to the electron flow, which substantially reduces the computational cost. The reasonability of numerical analyses using the hybrid model is largely dependent on the accuracy of the electron fluid calculation. The characteristics of the electron fluid in Hall thrusters is the high anisotropy owing to strong magnetic confinement. The large difference of electron mobilities between the tangential and orthogonal directions of magnetic lines of force makes the computation of the fluid difficult. The disparity of electron mobility causes a large condition number of the problem, which results in a slow convergence. Another issue is that a small numerical error in the computation may induce a large erroneous flux in along magnetic lines of force. There exists a demand of an efficient and accurate computational method which can cope with the issues of magnetized electron fluid.

One approach is to utilize a magnetic-field-aligned mesh (MFAM). In the MFAM, the boundary of each mesh is precisely aligned with tangential or orthogonal directions of the magnetic lines of force. The use of an MFAM is effective in reducing the numerical diffusion in the computation of magnetized electron fluid, and the MFAM has been used in various plasma simulations in electric propulsions.[4,8] Although the MFAM is effective in computing the magnetized electron fluid, it is not very compatible with the PIC method. The cell sizes in an MFAM typically significantly varies, especially in the magnetic field geometry of plasma lens focusing in Hall thrusters. In general, a minimum number of macro particles of ~ 50 must be maintained in each cell for calculation stability. In the MFAM, this criterion should be satisfied in the cell of minimum sizing. Therefore, if the PIC method is used in the MFAM, one needs to handle quite a number of macro particles in the calculation region, which results in a large computational cost. In terms of the compatibility with PIC methods, a simple mesh whose cell sizes are uniform or varying with plasma density, is preferred.

As an alternative approach for robust calculation of magnetized electron fluid, the hyperbolic-equation system (HES) approach has been proposed.[9] This approach avoids the treatment of cross-diffusion terms which appears in the diffusion equation, by constructing an HES with pseudo-time advancement terms. A preconditioning method is used for the pseudo-time advancement terms to solve the issue of large condition number due to the disparity of electron mobilities. Numerical diffusions are reduced by implementing a high-order space-accuracy method. The HES approach can utilize a simple structured mesh for calculating magnetized electron fluids such as the ones in Hall thrusters.[10] In previous researches, the effectiveness of the HES approach was examined by test calculations only for electron fluids. The applicability of the HES approach to the hybrid PIC method is yet to be proven.

The purpose of this paper is to discuss the applicability of the HES approach to a Hall thruster calculation using the hybrid PIC method. The applicability is examined by the following points: 1) conservation of electron flux, 2) satisfaction of Bohm criterion, and 3) the Boltzmann relation along magnetic lines of force in the region of strong magnetic confinement. Concerning point 1), strict conservations of numerical fluxes are expected by computing the HES by using the finite volume method. The point 2) evaluates how accurately the boundary condition of the wall sheath is implemented in the HES approach. The point 3) is expected if the HES approach reasonably calculate the magnetized electron fluid in Hall thrusters. The discussion is mainly focused on the verification, but not the validation.[11] Thus, simplified models are used for electron mobility and wall sheath, without losing the main characteristics of the Hall thruster discharge. The SPT-100 thruster is assumed for the calculation condition, since various data of experiments and numerical simulations are available.

II. Hyperbolic-Equation System Approach for Electron Fluid

In this section, an overview of the construction of the HES for magnetized electron fluids is explained. The fundamental equations are the two-dimensional conservation equations of electron mass, momentum, and energy in quasi-neutral plasmas. First of all, for the convenience of expression, the negative space potential is defined as follows:

$$\phi_{\mathrm{n}} = -\phi. \tag{1}$$

In the mass conservation equation, the electron number density is treated as a time-constant distribution by assuming the quasi-neutrality. Thus, the mass conservation equation is regarded as the equation of continuity as follows:

$$\nabla \cdot \left(n_{\mathrm{e}} \vec{u}_{\mathrm{e}}\right) = n_{\mathrm{e}} \nu_{\mathrm{ion}}. \tag{2}$$

Conservation of the electron momentum is derived by assuming inertialess electrons, as follows:

$$n_{\mathrm{e}} \left[\mu\right] \nabla \phi_{\mathrm{n}} + \left[\mu\right] \nabla \left(n_{\mathrm{e}} T_{\mathrm{e}}\right) = -n_{\mathrm{e}} \vec{u}_{\mathrm{e}}, \tag{3}$$

where the electron mobility tensor $[\mu]$ is given as follows:

$$\left[\mu\right] = \Theta^{-1} \left[\mu\right]_{\mathrm{mag}} \Theta, \tag{4}$$

$$\left[\mu\right]_{\mathrm{mag}} = \begin{bmatrix} \mu_{||} & \\ & \mu_{\perp} \end{bmatrix}, \qquad \Theta = \begin{bmatrix} \cos\theta & -\sin\theta \\ \sin\theta & \cos\theta \end{bmatrix}. \tag{5}$$

Here, Θ is the rotation matrix, with the angle between the magnetic lines of force and the computational mesh. A lot of models have been proposed for accurate expression of the mobility in the perpendicular direction of magnetic lines of force. Most of them take into account both of the classical diffusion and anomalous diffusion as follows:

$$\mu_{\perp} = \frac{\mu_{||}}{1 + \left(\mu_{||} B\right)^2} + \frac{\alpha_{\mathrm{B}}}{B}, \tag{6}$$

where α_{B} is the Bohm diffusion coefficient. It has been reported that the numerical simulation can reproduce the experimental results by spatially varying the Bohm diffusion coefficient. However, a consistent model for the anomalous diffusion is yet to be determined. Since the acquisition of an accurate electron mobility model is beyond the scope of this paper, an uniform Bohm diffusion coefficient of 1/64 is assumed in this calculation.[12]

In conventional approaches, Eq. (2) and Eq. (3) are integrated into an elliptic equation to solve for the space potential.[7] However, this equation becomes an anisotropic diffusion equation, and it is difficult to maintain a stability while computing this equation because the cross-diffusion terms cause failure of the diagonal dominance of the coefficient matrix.[9] Alternatively, the HES approach using pseudo-time advancement terms is considered. In quasi-neutral plasmas, the plasma approximation is assumed and the space potential is calculated from the conservation equations for the electrons.[13] Thus, a pseudo-time advancement term of space potential is introduced into the mass conservation equation as follows:

$$\frac{n_{\mathrm{e}}}{T_{\mathrm{e}}} \frac{\partial \phi_{\mathrm{n}}}{\partial t_{\mathrm{p}}} + \nabla \cdot \left(n_{\mathrm{e}} \vec{u}_{\mathrm{e}}\right) = n_{\mathrm{e}} \nu_{\mathrm{ion}}. \tag{7}$$

Eq. (3) is utilized to solve for the electron momenta as follows:

$$\frac{1}{\nu_{\mathrm{col}}} \frac{\partial}{\partial t_{\mathrm{p}}} \left(n_{\mathrm{e}} \vec{u}_{\mathrm{e}}\right) + n_{\mathrm{e}} \left[\mu\right] \nabla \phi_{\mathrm{n}} + \left[\mu\right] \nabla \left(n_{\mathrm{e}} T_{\mathrm{e}}\right) = -n_{\mathrm{e}} \vec{u}_{\mathrm{e}}. \tag{8}$$

In addition to the mass conservation and momentum conservation equations, the energy conservation equation is calculated to derive electron temperature. The electron energy conservation is formulated as follows:

$$\nabla \cdot \left(\frac{5}{2} e n_{\mathrm{e}} T_{\mathrm{e}} \vec{u}_{\mathrm{e}} - \frac{5}{2} e n_{\mathrm{e}} T_{\mathrm{e}} \left[\mu\right] \nabla T_{\mathrm{e}}\right) = \vec{j}_{\mathrm{e}} \cdot \vec{E} - \alpha e \varepsilon_{\mathrm{ion}} n_{\mathrm{e}} \nu_{\mathrm{ion}}, \tag{9}$$

where α is a coefficient to handle ionization, excitation, and radiation with a single term, and it is experimentally determined as a function of electron temperature.[14] It is assumed that the conservation of energy also achieves a steady state on the ion time scale.

Eq. (9) is modified to hyperbolic equations, since the heat conduction terms include anisotropic diffusion terms. First, the Joule heating is converted into the potential flux and potential gain by the electron production as follows:

$$\vec{j}_{\mathrm{e}} \cdot \vec{E} = e n_{\mathrm{e}} \vec{u}_{\mathrm{e}} \cdot \nabla \phi = -e n_{\mathrm{e}} \vec{u}_{\mathrm{e}} \cdot \nabla \phi_{\mathrm{n}} = -\nabla \cdot \left(e n_{\mathrm{e}} \phi_{\mathrm{n}} \vec{u}_{\mathrm{e}} \right) + e n_{\mathrm{e}} \phi_{\mathrm{n}} \nu_{\mathrm{ion}}. \tag{10}$$

To express Eq. (9) in a hyperbolic form, a pseudo-time advancement term of electron internal energy and new variables: $\vec{g} = -[\mu] \nabla T_{\mathrm{e}}$, are introduced. Then, Eq. (9) can be rewritten as follows:

$$\frac{\partial}{\partial t_{\mathrm{p}}} \left(\frac{3}{2} n_{\mathrm{e}} T_{\mathrm{e}} \right) + \nabla \cdot \left(\frac{5}{2} n_{\mathrm{e}} T_{\mathrm{e}} \vec{u}_{\mathrm{e}} + n_{\mathrm{e}} \phi_{\mathrm{n}} \vec{u}_{\mathrm{e}} + \frac{5}{2} n_{\mathrm{e}} T_{\mathrm{e}} \vec{g} \right) = \left(\phi_{\mathrm{n}} - \alpha \varepsilon_{\mathrm{ion}} \right) n_{\mathrm{e}} \nu_{\mathrm{ion}}. \tag{11}$$

The newly introduced variables $\vec{g}$ have the dimensions of velocity, and they are solved by using the pseudo-time advancement terms, as follows:

$$\frac{1}{\nu_{\mathrm{col}}} \frac{\partial \vec{g}}{\partial t_{\mathrm{p}}} + [\mu] \nabla T_{\mathrm{e}} = -\vec{g}. \tag{12}$$

Eventually, the HES consists of Eqs. (7), (8), (11), and (12). Upwind schemes based on the approximate Riemann solver can be constructed by using the Jacobian matrices of the hyperbolic system. This approach, using a first-order system, has originally been proposed by Nishikawa for future application to the Navier-Stokes equation.[15] This approach is expected to be beneficial for the computation of magnetized electrons because it avoids the difficulties associated with electron magnetization.

III. Numerical Method

The hybrid particle-in-cell (PIC) method treats ions and neutral particles as particles, whereas electrons are regarded as fluid. The overall calculation flow is visualized in Fig. 1. The computation mainly consists of two sections: PIC and fluid, which are described in detail in the following sections. Although the purpose of this calculation is to simulate the plasma behaviors in the steady thruster operation, it is difficult to define the steady state in Hall thrusters, since there exists several innate oscillation phenomena in Hall thrusters.[16]Thus, the time history of discharge current is observed, and the quasi-steady state is defined when cyclic behaviors are recognized. Then the time-averaged quantities during the cycle are visualized for the output.

III.A. Ions and Neutral Particles

The ionization collision frequency and total collision frequency are calculated by the following equations:

$$\nu_{\mathrm{ion}} = n_{\mathrm{n}} < \sigma_{\mathrm{ion}} v_{\mathrm{e,th}} >, \qquad \nu_{\mathrm{col}} = n_{\mathrm{n}} < \sigma_{\mathrm{col}} v_{\mathrm{e,th}} >, \tag{13}$$

where σ_{ion} and σ_{col} are the cross section of ionization collision and total collision. The cross-section data of various gases are given by experimental data. The electron thermal velocity is calculated based on the Maxwellian distribution regarding the electron temperature. Each reaction rate coefficient $< \sigma \nu >$ is approximated by a sixth-order polynomial function which is used in the coding. It is noted that only first-ionization of xenon is treated in this calculation. This is because the fraction of singly-charged ion is greater than 0.90 among the ion species in the SPT-100 plume,[17] and the treatment of singly-charged ions is supposed to be sufficient to reproduce the major characteristics of the SPT-100 thruster.

To simplify the calculation, the effect of ion magnetization is neglected, and the ion particles are accelerated only by the electric field. The equation of motion is normalized by defining representative quantities, and it is further modified for the cylindrical coordinate. In plasma PIC calculations, time-symmetric methods are preferred for the particle mover to avoid numerical heatings.[18] Thus, this calculation employs the leap-frog method, which produces a second-order accuracy in the particle orbit. A first-order particle weighting, or cloud-in-cell (CIC) model[19] is used for the weighting function in the PIC method. The number of macro particles is adjusted to make each cell contains ~ 75 macro particles averagely, and usually $\sim 10^5$ macro particles flow in the calculation region. The time step interval is also adjusted depending on the maximum speed of ion particle, and it is generally set as $\Delta t \sim 1.0 \times 10^{-8}$ s.

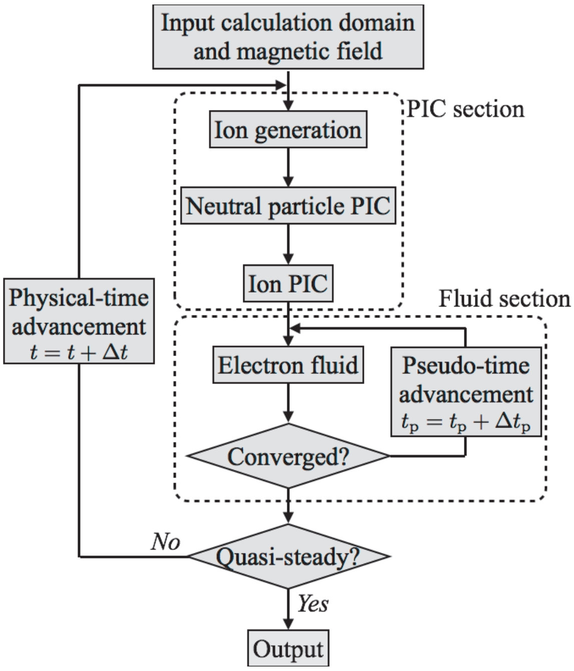

Figure 1. Calculation flow in the hybrid particle-in-cell (PIC) method using the HES approach.

III.B. Electrons

The HES consisting of Eqs. (7), (8), (11), and (12) is solved mainly for deriving space potential and electron temperature. First the system is modified to a dimensionless form by defining representative values for quantities such as electron number density and electron mean-free path. The flux Jacobian matrices in the HES is too complicated to analyze the eigen-structure, and hence it is difficult to develop an upwind method based on the characteristics of the full system. Alternatively, a flux-splitting method has been developed in which the numerical fluxes are split into several categories. The manner of splitting fundamentally follows the Nishikawa's approach in which the advection and diffusion Jacobian matrices are separated.[20] The flux categorization is also based on the concept of the advection upstream splitting method (AUSM).[21] The upwind direction of each flux is determined based on the characteristics of the split Jacobian matrices.

It is known that the discrepancy between the computational mesh and magnetic lines of force causes a large numerical viscosity.[4,22] In order to minimize the numerical viscosity, a third-order total variation diminishing monotonic upstream-centered scheme for conservation laws (TVD-MUSCL) technique is employed for the space discretization. Owing to the high-order scheme, a high computational accuracy can be obtained by using the HES approach.

The strong magnetic confinement for electrons results in a large condition number of the problem, which makes the convergence speed slow. To avoid the large condition number, a preconditioning matrix is multiplied to the pseudo-time advancement terms.[9] Basically the preconditioning matrix is designed to cancel the disparity of the electron mobilities between parallel and perpendicular directions of magnetic lines of force. Since the sub-loop in the electron fluid calculation is continued until the pseudo-time advancement terms become negligibly small values, the implicit time advancement should be employed to avoid the Courant-Friedrichs-Lewy (CFL) restriction. In this calculation, an implicit method based on the alternating-direction-implicit symmetric Gauss-Seidel (ADI-SGS) method[23] is implemented with a Courant number of 10.

IV. Calculation Condition

IV.A. Domain, Mesh, and Magnetic Field

The SPT-100 Hall thruster is assumed for the calculation condition. The input parameters are presented in Table 1 and the calculation region is illustrated in Fig. 2. A 56 $\times$ 21 rectangular mesh is used in the computation. This computational mesh is used in both of the PIC and electron fluid calculations. Since the quasi-neutrality is assumed in the hybrid model, the mesh size should be greater than the Debye length. For typical plasma parameters in Hall thrusters of $T_{\mathrm{e}} = 10$ eV and $n_{\mathrm{e}} = 10^{18}$ m^{-3}, the Debye length is calculated as $\lambda_{\mathrm{D}} = 0.024$ mm. Thus, the mesh size is approximately 30 times as large as the Debye length. The injector for xenon gas is distributed around the middle of the anode. Fig. 3 shows the magnetic field geometry and axial distribution of radial magnetic flux density. This magnetic field is generated referring to the magnetic field configuration of the SPT-100.[24]

Table 1. The input parameters assumed in the SPT-100 calculation.

Parameter	Value
Outer channel diameter, mm	50.0
Inner channel diameter, mm	35.0
Channel length, mm	23.0
Discharge voltage, V	300
Mass flow rate, mg s^{-1}	5.00
Wall temperature, K	850

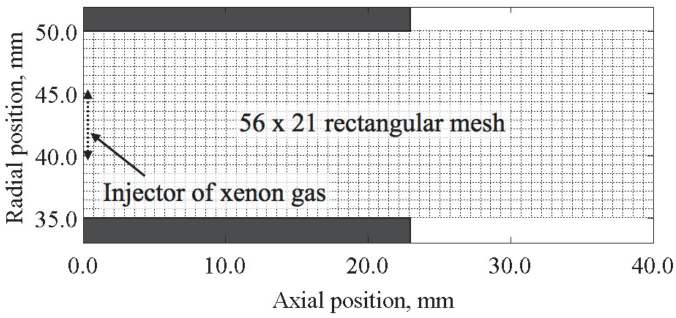

Figure 2. The calculation region and 56 $\times$ 21 computational mesh. The location of the injector is denoted in the figure.

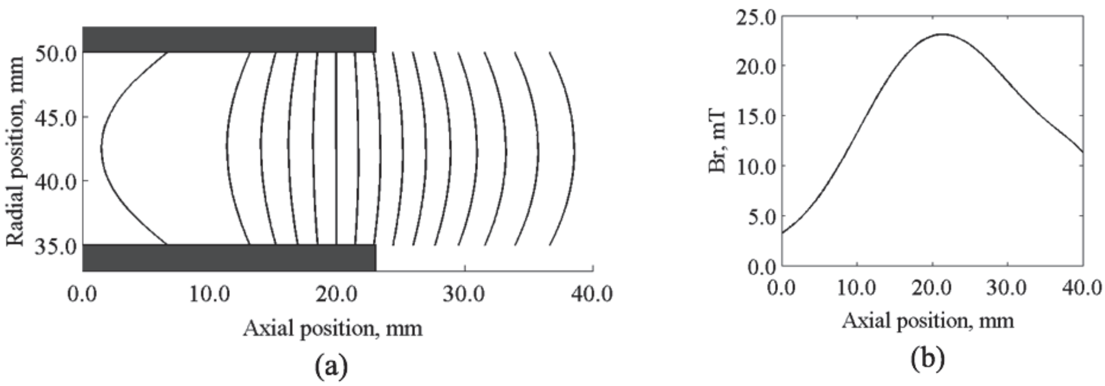

Figure 3. (a): Magnetic field geometry assumed in the calculation. (b): Axial distribution of radial magnetic flux density.

IV.B. Boundary Conditions

The boundary conditions for ions and neutral particles are illustrated in Fig. 4. The neutral xenon particles of the mass flow rate flow into the calculation region from the injector. All of the ions are generated in the calculation region with a random thermal speed based on the wall temperature. The neutral particles colliding with the channel wall or anode are reflected by the diffusion reflection, whereas ions are recombined to be neutrals.

Electron-repelling sheath is assumed for both the dielectric channel walls and anode. For stable sheath formation, the Bohm criterion is required to be satisfied. The Bohm criterion is simply imposed as a boundary condition as follows:[25]

$$n_{\mathrm{e,s}} = \frac{\Gamma_{\mathrm{i,s}}}{u_{\mathrm{Bohm}}}, \tag{14}$$

where u_{Bohm} is the Bohm velocity and $\Gamma_{\mathrm{i,s}}$ is calculated by the ion PIC calculation. The boundary conditions for electron fluid calculation is shown in Fig. 5. Simple boundary conditions of electrostatic sheath neglecting the effects of secondary electron emission (SEE) are used. At the plasma-sheath boundary in front of the channel walls, the ion and electron fluxes entering the sheath are balanced, thus,

$$(n_{\mathrm{e}} u_{\mathrm{e}})_{\mathrm{s}} = \Gamma_{\mathrm{i,s}}. \tag{15}$$

In front of the anode, it is assumed that an electron-repelling sheath is formed. The potential at the sheath boundary can be determined as follows:

$$\Gamma_{\mathrm{random,e,s}} \exp\left(\frac{\phi_{\mathrm{w}} - \phi_{\mathrm{s}}}{T_{\mathrm{e,s}}}\right) = \Gamma_{\mathrm{e,s}}, \qquad \text{where} \quad \Gamma_{\mathrm{random,e,s}} = \frac{1}{4} n_{\mathrm{e,s}} \sqrt{\frac{8}{\pi}\frac{eT_{\mathrm{e,s}}}{m_{\mathrm{e}}}}. \tag{16}$$

ϕ_{w} is given as a discharge voltage. Eq. (16) yields the boundary condition for the plasma-sheath boundary in front of the anode as follows:

$$\phi_{\mathrm{s}} = \phi_{\mathrm{w}} - T_{\mathrm{e,s}} \ln\left(\frac{\Gamma_{\mathrm{e,s}}}{\Gamma_{\mathrm{random,e,s}}}\right) \tag{17}$$

Generally, $\Gamma_{\mathrm{e,s}} < \Gamma_{\mathrm{random,e,s}}$,[26] and hence $\phi_{\mathrm{s}} > \phi_{\mathrm{w}}$. Then, $\phi = \phi_{\mathrm{s}}$ is used for the boundary condition for electron conservation. In the code, Eq. (17) is implemented with a pseudo-time relaxation. Since the zero-SEE condition is assumed, the energy fluxes flowing into the walls are always associated with electron fluxes. Thus, the boundary condition for the energy conservation equation at the channel walls and anode is a Dirichlet condition as follows:

$$g_{\mathrm{s}} = 0. \tag{18}$$

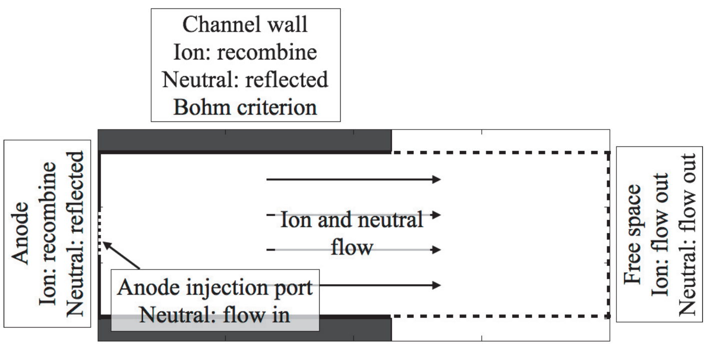

Figure 4. The boundary conditions for ion and neutral particles.

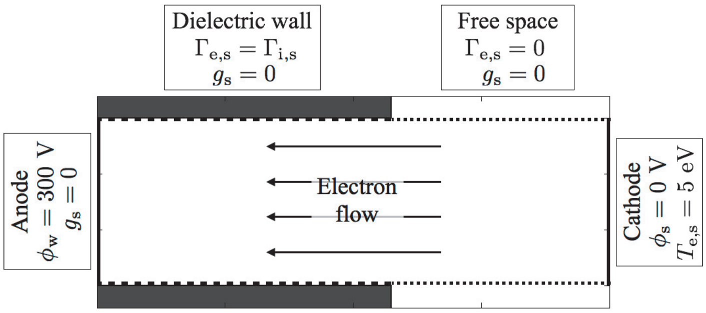

Figure 5. The boundary conditions for electron fluid.

V. Results and Discussion

V.A. Overview of Calculation Results

The calculation of 1.0 ms discharge is completed within 5 hr in wall-clock time, by using a 6-core 3.2 GHz workstation. This efficient calculation is enabled owing to the preconditioning and implicit methods in the HES approach. First of all, the calculated thruster performance is compared with experimental values in Table 2. The difference between the calculated and experimental values are within 6%. The reason of this discrepancy is that the electron mobility model is yet to be tuned to match the calculation results with experiments. Nonetheless, the hybrid PIC method with the HES approach is able to reproduce the major characteristics of the Hall thruster discharge. The two-dimensional distributions of various plasma properties are visualized in Fig. 6. The equipotential lines in Fig. 6-(a) are distorted by the presence of a presheath. Ions are attracted to the channel walls by the presheath, and recombined to be neutral particles. Owing to the increased neutral number density in front of the channel walls, the region of high ion-production rate expands to the channel walls as shown in Fig. 6-(e), in the current calculation. The peak values of electron number density and electron temperature are 1.6×10^{18} m^{-3} and 25 eV, respectively. Similar values were observed in the simulation results of SPT-100 by the HPHall-2 code.[27]

V.B. Strict Conservation of Electron Flux

Since the HES approach is based on the finite volume method, strict conservations of numerical fluxes are expected. This section discusses the attainment level of the electron flux conservation. The electron current balance in the calculation region is presented in Table 3. The error of electron current balance at one time step was 2.2×10^{-3} A. This quite small error of electron current conservation is maintained during the calculation. Therefore, it is confirmed that strict conservation of electron flux is achieved by the HES approach. Another results which support the strictness of flux conservation are the electron streamlines shown in Fig. 7. In the calculation of magnetized electron fluid, a small residual in the computation may induce a large erroneous flux in the parallel direction of magnetic lines of force. The smooth electron streamlines in Fig. 7 indicate that the residuals are small in all the calculation region, and the flux conservations are attained.

Table 2. Thruster performance of SPT-100 from the experiment and calculation results.

	Experiment[27]	Calculation	Error
Discharge current, A	4.5	4.3	-4.4%
Thrust, mN	85	82	-3.5%
Anode efficiency	0.55	0.52	-5.5%
Specific impulse, s	1780	1680	-5.6%

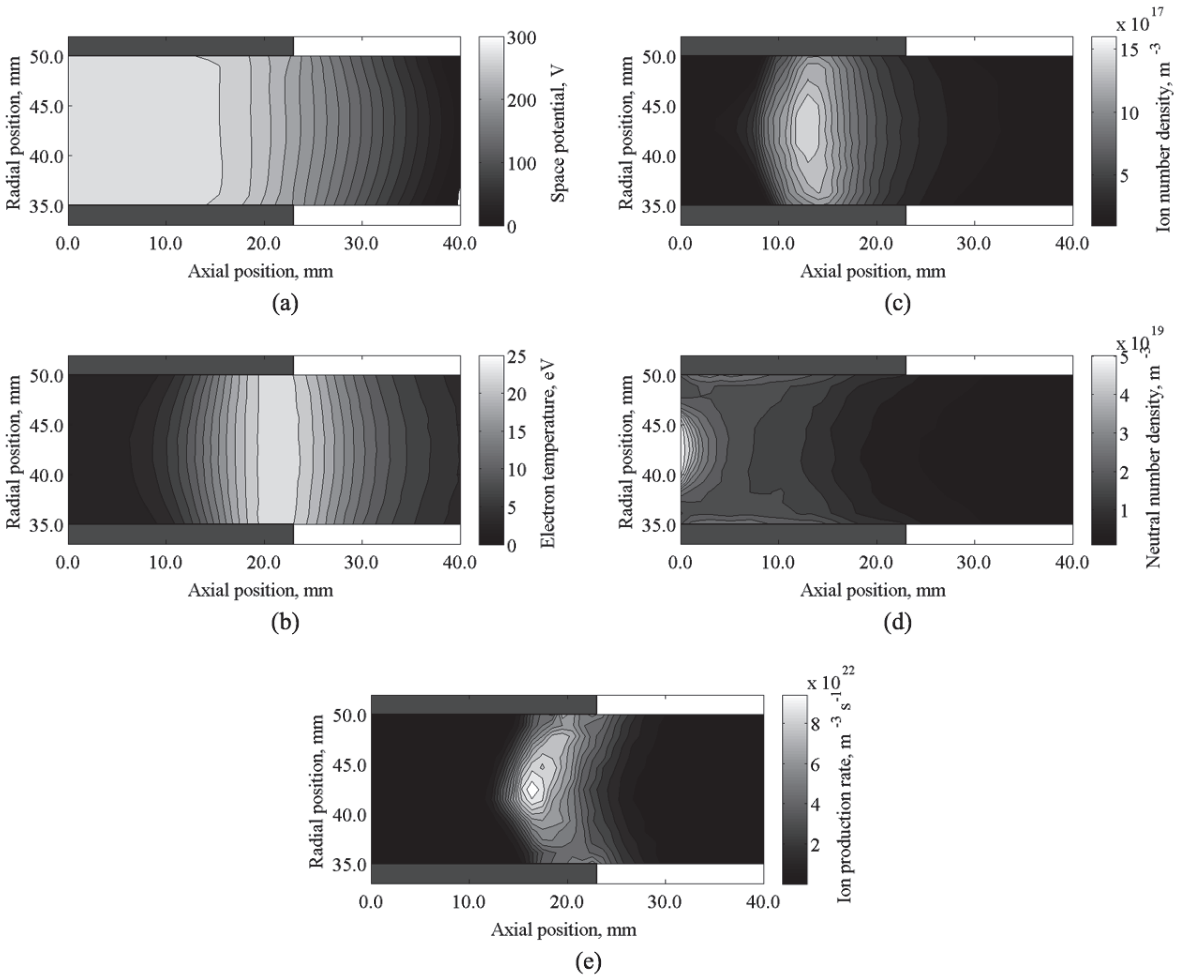

Figure 6. Two-dimensional distribution of plasma properties. (a): Space potential. (b): Electron temperature. (c): Ion number density. (d): Neutral number density. (e): Ion production rate.

Table 3. Electron current balance in the calculation region at one time step. The plus and minus denote inflow and outflow, respectively.

Anode	Inner wall	Outer wall	Cathode	Generation	Error
-4.31 A	-0.69 A	-0.99 A	1.81 A	4.19 A	2.2×10^{-3} A

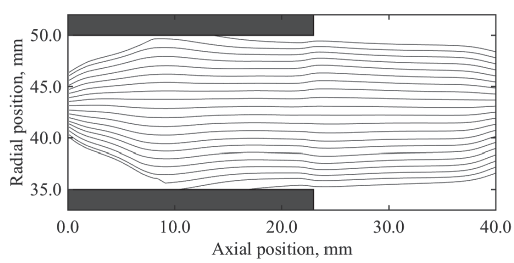

Figure 7. Electron streamlines calculated by the HES approach for electron fluid.

V.C. Satisfaction of the Bohm Criterion

As expressed in Eq. (14), the boundary condition using the Bohm criterion is imposed on the electron number density at the plasma-sheath boundary. If this condition is accurately reflected to the presheath formation, the ion velocity entering sheath should have the Bohm velocity. The average ion velocity entering sheath calculated by the PIC method and the Bohm velocity are compared in Fig. 8 for the inner and outer channel walls. The Bohm velocity is attained at both of the inner and outer channel walls by the average ion velocity calculated by the PIC method. This fact verifies that the hybrid modeling using the HES approach achieves a good accuracy in analyzing the effect of presheath. In this paper, the simple boundary condition of Eq. (14) is used. Even if the boundary condition is revised to include the effect of SEE, the HES approach is expected to reflect the boundary condition of wall sheath to the plasma dynamics appropriately.

V.D. Confirmation of the Boltzmann Relation Along Magnetic Lines of Force

The Boltzmann relation along magnetic lines of force is expected in the region of strong magnetic confinement. The strength of magnetic confinement for electron fluid is associated with the electron Hall parameter. The axial distribution of the Hall parameter at the channel centerline is shown in Fig. 9. In the evaluation of the attainment of the Boltzmann relation, the three regions of (a) near-anode region, (b) channel-exit region, and (c) plume region, are defined as denoted in Fig. 9. In the (b) and (c) regions, the electron Hall parameter exceeds 50, and hence the electron motions are strongly confined by the magnetic field.

The Boltzmann relation can be interpreted as the property of uniform thermalized potential as follows:

$$\phi_{\mathrm{th}} = \phi - T_{\mathrm{e}} \ln (n_{\mathrm{e}}) = \mathrm{const.} \tag{19}$$

Equipotential lines of the thermalized potential are compared with magnetic lines of force in Fig. 10. The equipotential lines of the thermalized potential are fairly aligned with the magnetic lines of force in the regions of (b) and (c). Thus, the property of Eq. (19) is satisfied in the region of strong magnetic confinement. It is concluded that the HES approach reasonably calculates the magnetized electron fluid with the simple rectangular mesh.

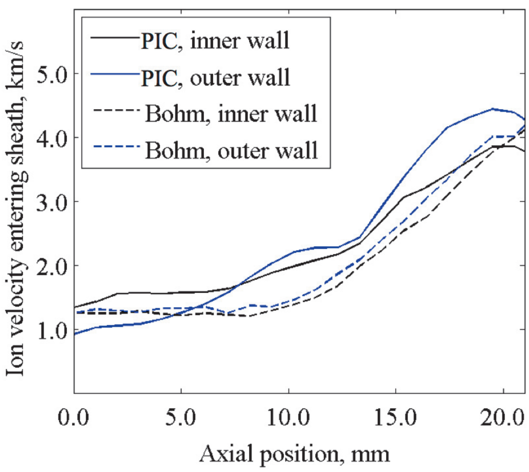

Figure 8. Comparison between average ion velocity entering sheath by the PIC calculation and the Bohm velocity for the inner and outer channel walls.

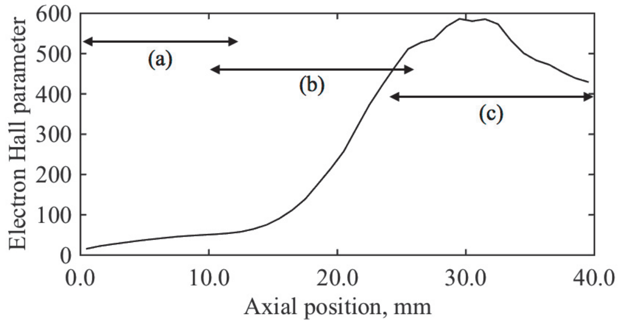

Figure 9. The axial distribution of the calculated Hall parameter at the channel centerline. Three regions of (a) near-anode region, (b) channel-exit region, and (c) plume region, are defined. Strong magnetic confinement is expected in the (b) and (c) regions.

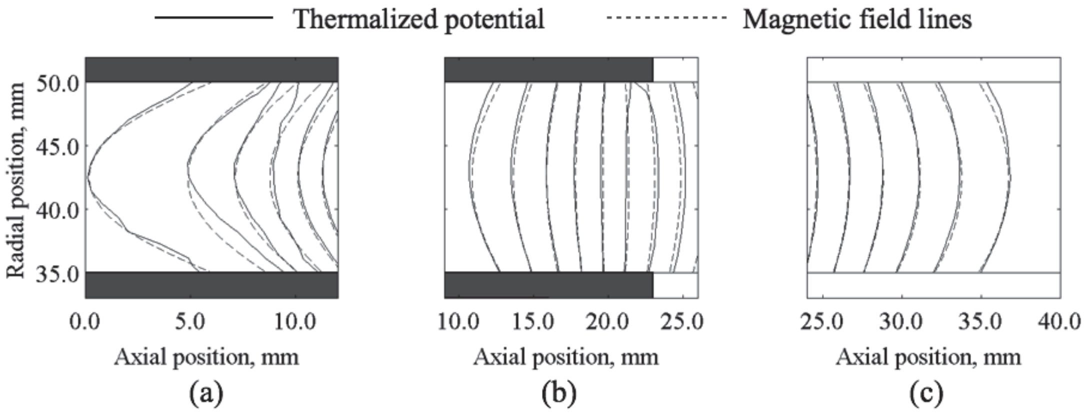

Figure 10. The distributions of equipotential lines of thermalized potential and magnetic lines of force. (a): Near-anode region. (b): Channel-exit region. (c): Plume region. The Boltzmann relation along magnetic lines of force are confirmed in the (b) and (c) regions.

VI. Conclusion

The HES approach was applied to the calculation of a Hall thruster using the hybrid PIC method. The HES approach is able to calculate the two-dimensional conservation equations of magnetized electron fluid with a simple structured mesh. The SPT-100 thruster was assumed as the calculation condition in which the simple models of electron mobility and electrostatic sheath were used. The findings are summarized as follows:

1. The hybrid PIC method using the HES approach is able to reproduce the fundamental characteristics of the Hall thruster discharge.

2. Electron fluxes are strictly conserved in the HES approach during the calculation of the hybrid PIC method.

3. The Bohm criterion was satisfied at the plasma-sheath boundary in front of the channel walls. This fact indicates that the HES approach accurately reflects the boundary conditions of the wall sheath to the plasma dynamics.

4. The Boltzmann relation along magnetic lines of force was confirmed in the strong magnetic confinement region. The HES approach reasonably calculates the magnetized electron fluid in the Hall thruster with simple rectangular mesh.

Based on the findings above, it is concluded that the HES approach is applicable to Hall thruster simulations using the hybrid PIC method, where the boundary condition of the sheath model is accurately implemented.

References

[1]Goebel, D. M. and Katz, I., *Fundamentals of Electric Propulsion: Ion and Hall Thrusters*, Johm Wiley & Sons, New Jersey, 2008.

[2]Cho, S., Komurasaki, K., and Arakawa, Y., "Kinetic particle simulation of discharge and wall erosion of a Hall thruster," *Physics of Plasmas*, Vol. 20, No. 6, 2013, pp. 063501.

[3]Garrigues, L., Hagelaar, G. J. M., Bareilles, J., Boniface, C., and Boeuf, J. P., "Model study of the influence of the magnetic field configuration on the performance and lifetime of a Hall thruster," *Physics of Plasmas*, Vol. 10, No. 12, 2003, pp. 4886 – 4892.

[4]Mikellides, I. G., Katz, I., Hofer, R. R., Goebel, D. M., de Grys, K., and Mathers, A., "Magnetic shielding of the channel walls in a Hall plasma accelerator," *Physics of Plasmas*, Vol. 18, No. 3, 2011, pp. 033501.

[5]Hofer, R. R., Goebel, D. M., Mikellides, I. G., and Katz, I., "Magnetic shielding of a laboratory Hall thruster. II. Experiments," *Journal of Applied Physics*, Vol. 115, No. 4, 2014, pp. 043304.

[6]Mikellides, I. G., Katz, I., Hofer, R. R., and Goebel, D. M., "Magnetic shielding of a laboratory Hall thruster. I. Theory and validation," *Journal of Applied Physics*, Vol. 115, No. 4, 2014, pp. 043303.

[7]Komurasaki, K. and Arakawa, Y., "Two-dimensional numerical model of plasma flow in a Hall thruster," *Journal of Propulsion and Power*, Vol. 11, No. 6, 1995, pp. 1317 – 1323.

[8]Wirz, R. and Katz, I., "A Preliminary 2-D Computational Model of an Ion Thruster Discharge Chamber," 39th Joint Propulsion Conference and Exhibit, AIAA 2003-5163, 2003.

[9]Kawashima, R., Komurasaki, K., and Schönherr, T., "A hyperbolic-equation system approach for magnetized electron fluids in quasi-neutral plasmas," *Journal of Computational Physics*, Vol. 284, 2015, pp. 59–69.

[10]Kawashima, R., Komurasaki, K., and Koizumi, H., "Modeling of Electron Fluids in Hall Thrusters Using a Hyperbolic System," 50th Joint Propulsion Conference, AIAA 2014-3622, 2014.

[11]Thacker, B. H., Doebling, S. W., Hemez, F. M., Anderson, M. C., Pepin, J. E., and Rodriguez, E. A., *Concepts of model verification and validation*, No. LA-14167, Los Alamos National Laboratory, 2004.

[12]Cho, S., Komurasaki, K., and Arakawa, Y., "Lifetime Simulation of a SPT-Type Hall Thruster by Using a 2D Fully Kinetic PIC Model," 48th Joint Propulsion Conference and Exhibit, AIAA 2012-4016, 2012.

[13]Chen, F. F., *Introduction to plasma physics and controlled fusion*, Plenum Press, New York, 1984.

[14]Dugan, J. J. and Sovie, R., "Volume Ion Production Costs in Tenuous Plasmas: a General Atom Theory and Detailed Results for Helium, Argon, and Cesium," NASA Technical Note, D-4150, 1967.

[15]Nishikawa, H., "A first-order system approach for diffusion equation. I: Second-order residual-distribution schemes," *Journal of Computational Physics*, Vol. 227, No. 1, 2007, pp. 315 – 352.

[16]Choueiri, E. Y., "Plasma oscillations in Hall thrusters," *Physics of Plasmas*, Vol. 8, No. 4, 2001, pp. 1411–1426.

[17]Kim, S.-W. and Gallimore, A. D., "Plume Study of a 1.35-kW SPT-100 Using an ExB Probe," *Journal of Spacecraft and Rockets*, Vol. 39, No. 6, 2002, pp. 904–909.

[18]Buneman, O., "Time-reversible difference procedures," *Journal of Computational Physics*, Vol. 1, No. 4, 1967, pp. 517 – 535.

[19]Birdsall, C. K. and Langdon, A. B., *Plasma physics via computer simulation*, CRC Press, 2004.

[20]Nishikawa, H., "A first-order system approach for diffusion equation. II: Unification of advection and diffusion," *Journal of Computational Physics*, Vol. 229, No. 11, 2010, pp. 3989 – 4016.

[21]Liou, M.-S., "A Sequel to AUSM: AUSM+," *Journal of Computational Physics*, Vol. 129, No. 2, 1996, pp. 364 – 382.

[22]Hagelaar, G. J. M., "Modelling electron transport in magnetized low-temperature discharge plasmas," *Plasma Sources Science and Technology*, Vol. 16, No. 1, 2007, pp. S57.

[23]Nishida, H. and Nonomura, T., "ADI-SGS scheme on ideal magnetohydrodynamics," *Journal of Computational Physics*, Vol. 228, No. 9, 2009, pp. 3182 – 3188.

[24]Mitrofanova, O. A., Gnizdor, R. Y., Murashko, V. M., Koryakin, A. I., and Nesterenko, A. N., "New Generation of SPT-100," 32nd International Electric Propulsion Conference, IEPC-2011-041, 2011.

[25]Parra, F. I. and Ahedo, E., "Fulfillment of the Bohm condition on the 'HPHall' fluid-PIC code," 40th Joint Propulsion Conference and Exhibit, AIAA 2004-3955, 2004.

[26]Fife, J. M., "Hybrid-PIC Modeling and Electrostatic Probe Survey of Hall Thrusters," Ph.D. Thesis, Massachusetts Institute of Technology, 1998.

[27]Hofer, R., Mikellides, I., Katz, I., and Goebel, D., "Wall Sheath and Electron Mobility Modeling in Hybrid-PIC Hall Thruster Simulations," 43rd Joint Propulsion Conference and Exhibit, AIAA 2007-5267, 2007.